

## ON THE CORRELATION BETWEEN SPIN PARAMETER AND HALO MASS

ALEXANDER KNEBE<sup>1</sup>, CHRIS POWER<sup>2</sup>

*Draft version August 9, 2021*

### ABSTRACT

We report on a correlation between virial mass  $M$  and spin parameter  $\lambda$  for dark matter halos forming at redshifts  $z \gtrsim 10$ . We find that the spin parameter decreases with increasing halo mass. Interestingly, our analysis indicates that halos forming at later times do not exhibit such a strong correlation, in agreement with the findings of previous studies. We briefly discuss the implications of this correlation for galaxy formation at high redshifts and the galaxy population we observe today.

*Subject headings:* galaxies: formation — cosmology: theory — cosmology: early Universe — methods: numerical

### 1. INTRODUCTION

The physical mechanism by which galaxies acquire their angular momentum is an important problem that has been the subject of investigation for nearly sixty years (Hoyle 1949). This reflects the fundamental role played by angular momentum of galactic material in defining the size and shapes of galaxies (e.g. Fall & Efstathiou 1981). Yet despite its physical significance, a precise and accurate understanding of the origin of galactic angular momentum remains one of the missing pieces in the galaxy formation puzzle.

A fundamental assumption in current galaxy formation models is that galaxies form when gas cools and condenses within the potential wells of dark matter halos (White & Rees 1978). Consequently it is probable that the angular momentum of the galaxy will be linked to the angular momentum of its dark matter halo (e.g. Fall & Efstathiou 1980; Mo, Mao & White 1998; Zavala, Okamoto & Frenk 2007). Within the context of hierarchical structure formation models, the angular momentum growth of a dark matter proto-halo is driven by gravitational tidal torquing during the early stages (i.e. the linear regime) of its assembly. This “Tidal Torque Theory” has been explored in detail; it is a well-developed analytic theory (e.g. Peebles 1969, Doroshkevich 1979, White 1984) and its predictions are in good agreement with the results of cosmological  $N$ -body simulations (e.g. Barnes & Efstathiou 1987; Warren et al. 1992; Sugerman, Summers & Kamionkowski 2000; Porciani, Dekel & Hoffman 2002). However, once the proto-halo has passed through maximum expansion and the collapse has become non-linear, tidal torquing no longer provides an adequate description of the evolution of the angular momentum (White 1984), which tends to decrease with time. During this phase it is likely that merger and accretion events play an increasingly important role in determining both the magnitude and direction of the angular momentum of a galaxy (e.g. Bailin & Steinmetz 2005). Indeed, a number of studies have argued that mergers and accretion events are the primary determinants of the angular momenta of galaxies at the present day (Gardner 2001; Maller, Dekel & Somerville 2002; Vitvitska et al. 2002).

It is common practice to quantify the angular momentum of a dark matter halo by the dimensionless “classical” spin param-

eter (Peebles 1969),

$$\lambda = \frac{J\sqrt{|E|}}{GM^{5/2}}, \quad (1)$$

where  $J$  is the magnitude of the angular momentum of material within the virial radius,  $M$  is the virial mass, and  $E$  is the total energy of the system. It has been shown that halos that have suffered a recent major merger will tend to have a higher spin parameter  $\lambda$  than the average (e.g. Hetzner & Burkert 2006; Power, Knebe & Knollmann 2008). Therefore one could argue that within the framework of hierarchical structure formation that higher mass halos should have larger spin parameters *on average* than less massive systems because they have assembled a larger fraction of their mass (by merging) more recently.

However, if we consider only halos in virial equilibrium, should we expect to see a correlation between halo mass and spin? One might naïvely expect that more massive systems will have had their maximum expansion more recently and so these systems will have been tidally torqued for longer than systems that had their maximum expansion at earlier times. This suggests that spin should *increase* with timing of maximum expansion and therefore halo mass. However, one finds at best a weak correlation between mass and spin for equilibrium halos at  $z=0$  (e.g. Cole & Lacey 1996; Maccio et al. 2007; Bett et al. 2007, hereafter B07), and the correlation is for spin to *decrease* with increasing halo mass, contrary to our naïve expectation.

In this paper, we report on a (weak) correlation between spin and mass for equilibrium halos at redshift  $z=10$ . The trend is for higher-mass halos to have smaller spins, and is qualitatively similar to the one reported by B07 for the halo population at  $z=0$ . We present the main evidence in support of this correlation in Section 4 and we consider its implications for galaxy formation in Section 6.

### 2. THE SIMULATIONS

For the simulations presented in this paper we have adopted the cosmology as given by Spergel et al. (2003) ( $\Omega_0 = 0.3$ ,  $\Omega_\Lambda = 0.7$ ,  $\sigma_8 = 0.9$ , and  $H_0 = 70$  km/sec/Mpc). Each run employed  $N = 256^3$  particles and differed in simulation box-size  $L_{\text{box}}$ , which leads to the particle mass  $m_p$  differing between runs  $- m_p = \rho_{\text{crit}}\Omega_0(L_{\text{box}}/N)^3$ , where  $\rho_{\text{crit}} = 3H_0^2/8\pi G$ . This allows us to probe a range of halo masses at redshift  $z=10$ . The primary parameters of these simulations are summarized in Table 1.

<sup>1</sup>Astrophysikalisches Institut Potsdam, An der Sternwarte 16, 14482 Potsdam, Germany

<sup>2</sup>Centre for Astrophysics & Supercomputing, Swinburne University, Mail H31, PO Box 218, Hawthorn, VIC 3122, Australia

Halos in all runs have been identified using the MPI parallelized version of the AHF halo finder<sup>3</sup> (AMIGA’s-Halo-Finder), which is based on the MHF halo finder of Gill, Knebe & Gibson (2004). For each halo we compute the virial radius  $R$ , defined as the radius at which the mean interior density is  $\Delta_{\text{vir}}$  times the background density of the Universe at that redshift. This leads to the following definition for the virial mass  $M$ :

$$M = \frac{4\pi}{3} \Delta_{\text{vir}} \Omega \rho_{\text{crit}} R^3. \quad (2)$$

Note that  $\Delta_{\text{vir}}$  is a function of redshift and amounts to  $\Delta_{\text{vir}} \approx 210$  at redshift  $z=10$ ,  $\Delta_{\text{vir}} \approx 230$  at  $z=1$ , and the “usual”  $\Delta_{\text{vir}} \approx 340$  at  $z=0$  (cf. Gross 1997). Table 1 summarises the total number of halos ( $N_{\text{halos}}$ ) recovered by AHF, while  $z_{\text{final}}$  gives the redshift that the simulation has been evolved to.

We add that we ran five realisations of B20 to redshift  $z=10$  in order to have a statistically significant sample of halos in that particular model. However, we also note that the fitting parameters presented in the following Section are robust in the sense that they do not depend on whether we stack the halos from those five runs or use them individually.

### 3. THE HALO SAMPLE

We show in a companion paper (Power, Knebe & Knollmann 2008) that a substantial fraction of the halo population at high redshift is not in virial equilibrium. Because we wish to examine the spin distribution of equilibrium halos, it is important to account for unrelaxed systems when investigating correlations between spin and halo mass. For example, it has been shown that the spin can increase sharply in the aftermath of mergers with mass ratios as modest as 5:1 (e.g. Hetzner & Burkert 2006), and that the degree to which a halo is in dynamical relaxation is as important as recent merging history in its influence on spin (D’Onghia & Navarro 2007). To ensure that halos in our sample are in virial equilibrium, we compute the virial ratio for each halo, which we define as

$$Q = \frac{2T + S_p}{U} + 1. \quad (3)$$

Here  $T$  represents the kinetic energy,  $U$  the potential energy, and  $S_p$  the surface pressure of a given halo of mass  $M$ . By including  $S_p$ , we can account for the effect of infalling material on the dynamical state of the halo. Each of these quantities are evaluated using all gravitationally bound particles, and we adopt the formula of Shaw et al. (2006) for the surface pressure term  $S_p$  (cf. equations.(4)-(6) in their study).

In Figure 1 we show that the relation between halo mass and  $Q$  can vary with mass. This is apparent at redshift  $z=1$ , where we find a trend for more massive halos to be less virialised. In contrast, high redshift halos are less virialised on average (as indicated by the increased average  $\langle Q \rangle \approx -0.3$ ), but we find no apparent trend with mass.

Why is there a mass dependence at  $z=1$  but not at  $z=10$ ? There are two factors. The first is that high redshift halos “see” an effective slope of the initial power spectrum of  $n_{\text{eff}} \approx -3$ , and so the time at which a particular mass scale starts to collapse is relatively insensitive to mass. Therefore we do not expect to find a strong correlation between virial state  $Q$  and mass. We have checked this halo populations drawn from the simulations of scale-free cosmologies of Knollmann, Power & Knebe

(2008) and our interpretation is consistent with the correlations we find in these runs. The second is that the typical collapsing mass  $M^*$  at  $z=10$  is small – of order  $10^3 h^{-1} M_{\odot}$  – and because we resolve mass scales that have collapsed more or less simultaneously, we see a population that has yet to relax. At  $z=1$ , the typical collapsing mass is much larger – of order  $10^{11} h^{-1} M_{\odot}$  – and so we resolve a population of halos whose mass accretion histories are more diverse. The most massive systems tend to be ones that have formed most recently, and are therefore the least dynamically relaxed.

We have used the following relation between  $Q$  and  $M$  to classify dynamically relaxed and unrelaxed systems:

$$\begin{aligned} Q_{\text{allowed}} &\propto M^{-0.015}, & \text{for } z = 1 \\ Q_{\text{allowed}} &\propto \text{const.}, & \text{for } z = 10 \end{aligned} \quad (4)$$

We allow the  $Q$  values of halos in our sample to deviate from these scaling relations by not more than

$$Q_{\text{allowed}} - Q_{\text{lim}} \leq Q \leq Q_{\text{allowed}} + Q_{\text{lim}} \quad (5)$$

with  $Q_{\text{lim}} = 0.15$  (indicated by the dashed lines in Fig. 1). Furthermore, we consider only halos that contain at least  $N_{\text{min}} = 600$  particles within their virial radius to ensure that we are not influenced by particle discreteness. Interestingly, when computing spin, the tightest restriction on particle number comes not from the calculation of angular momentum but from the calculation of the potential energy. By comparing analytic solutions with Monte Carlo realisations of Navarro, Frenk & White (1997) haloes, we find that at least 600 particles are required if the energy is to be computed to better than 10%.

### 4. THE SPIN-MASS CORRELATION

Calculating the total energy  $E$  of a halo is computationally expensive, and so computing  $\lambda$  using Eq. (1) is also expensive. This prompted Bullock et al. (2001) to introduce a modified spin parameter

$$\lambda' = \frac{J}{\sqrt{2} M V R}, \quad (6)$$

where  $V = \sqrt{GM/R}$  measured the circular velocity at the virial radius  $R$  and  $J$  represents the absolute value of the angular momentum. We follow Bullock et al. and compute spin using equation (6).

In Figure 2, we investigate the correlation between halo spin  $\lambda'$  and mass  $M$ . We show only halos that fulfill our selection criteria (individual dots) and bin the data in five mass bins equally spaced in log-space between  $M_{\text{min}}$  and  $M_{\text{max}}$  of the considered halos at the respective redshift. The values plotted as histograms thereby represent the weighted mean of all spin parameters in the respective mass range where the weight is inversely proportional to the error estimate

$$\frac{\sigma_J}{J} = \frac{0.2}{\lambda' \sqrt{N}} \quad (7)$$

for the spin parameter of a halo consisting of  $N$  particles as derived in Bullock et al. (2001) (cf. equation (7) in that study). The error bars indicate the standard deviation of the spin parameter values in the bin from the weighted mean.<sup>4</sup>

The best fitting power-laws to these histograms reveal that

<sup>3</sup>AHF is already freely available from <http://www.aip.de/People/aknebe>

<sup>4</sup>We like to note in passing that we also performed all of the analysis and stability checks using the median and the scatter about the median in each bin. The results remain unaffected and we therefore decide to only list them for the weighted means.

$$\lambda' \propto M^\alpha \quad (8)$$

with

$$\begin{aligned} \alpha &= -0.002 \pm 0.149, \text{ for } z=1 \\ \alpha &= -0.059 \pm 0.171, \text{ for } z=10. \end{aligned} \quad (9)$$

This indicates that there is a *weak* correlation at high redshifts for spin to decrease with increasing mass, albeit stronger than the one at  $z=1$ . We compute Spearman rank correlation coefficients at  $z=10$  (1) and find  $R_s = -0.137(0.06)$ .

As an alternative approach, we fit a lognormal function to each of our halo samples at  $z=10$  and  $z=1$ ,

$$P(\lambda') = \frac{1}{\lambda' \sqrt{2\pi} \sigma_0} \exp\left(-\frac{\ln^2(\lambda'/\lambda'_0)}{2\sigma_0^2}\right). \quad (10)$$

The resulting curves are presented in Fig. 3 whereas the best-fit parameters, median values for  $\lambda'_{\text{med}} = \text{median}(\lambda')$  and median halo masses  $M_{\text{med}}$  are given in Table 2. Inspection of the best-fit parameters confirm that the median spin declines as we move from less massive to more massive objects at high redshift.

## 5. STABILITY OF RESULTS

Because of the weak nature of the measured correlation it is vitally important to check its credibility by performing a statistical analysis. To this extent we investigate the sensitivity of the logarithmic slope  $\alpha$  with respect to a number of parameters that enter into its determination, namely the number of bins  $N_{\text{bins}}$  used for the histograms; the virialisation criterion parametrized via  $Q_{\text{lim}}$ ; and the minimum number of particles  $N_{\text{min}}$  within a halo's virial radius. Note that we vary one parameter at a time, keeping the others at their fixed ‘‘standard’’ values. The results are presented in Table 3, Table 4, and 5.

We find that bin number has practically no effect on the slope. Similarly we find that varying the virialisation criterion  $Q_{\text{lim}}$  has little effect on the slope of the relation between mass and spin, regardless of redshift (Table 4). In contrast, we find that the minimum number of particles within a halo's virial radius has a strong and systematic effect on the result at  $z=1$  – as  $N_{\text{min}}$  increases, we find that the logarithmic slope becomes shallower. This does not appear to be true at high redshift, although as we go to earlier times we find that the number of massive haloes becomes progressively smaller and our determination of  $\alpha$  becomes increasingly unreliable.

These tests lead us to believe that our results are both stable and reliable, and our main result holds: *the correlation between spin parameter  $\lambda'$  and halo mass  $M$  is one order of magnitude larger at redshift  $z=10$  than at  $z=1$ .*

As a further test of the credibility of the correlation we measure between halo mass and spin, we use the criteria of three other studies to select our halo sample. These are:

- Maccio et al. (2007) criteria:

- $N_{\text{min}} = 250$
- $x_{\text{off}} < 0.04$
- $\rho_{\text{rms}} < 0.4$

- Bett et al. (2007) criteria:

- $N_{\text{min}} = 300$

$$- Q_{\text{lim}} = 0.5$$

- Neto et al. (2007) criteria:

- $N_{\text{min}} = 600$
- $x_{\text{off}} < 0.07$
- $f_{\text{sub}} < 0.1$

Here  $N_{\text{min}}$  is again the minimum number of particles in a halo,  $Q_{\text{lim}}$  the virial limit as defined in Eq. (5),  $x_{\text{off}}$  measures the distance between the most bound particle and the centre of mass in units of the virial radius,  $\rho_{\text{rms}}$  is an indicator of how well the density profile of the halo can be fitted by a Navarro, Frenk & White (1997) profile (cf. Eq. (2) in Maccio et al. 2007), and  $f_{\text{sub}}$  is the fraction of mass in subhalos. The resulting power law slopes  $\alpha$  (cf. Eq. (8)) for  $z=1$  and  $z=10$  are presented in Table 6. Again we note that there appears to be a much stronger correlation between  $\lambda'$  and  $M$  at higher redshift. While the relation is consistent with zero at  $z=1$  (as confirmed by Maccio et al. 2007) spin and mass are correlated at  $z=10$ . How this result relates to the Bett et al. (2007) result – who find a weak correlation at  $z=0$  – will be discussed in the following Section.

## 6. CONCLUSIONS AND DISCUSSION

We have performed a careful investigation of the relation between virial mass and dimensionless spin parameter for dark matter halos forming at high redshifts  $z \gtrsim 10$  in a  $\Lambda$ CDM cosmology. The result of our study, which is based on a series of cosmological  $N$ -body simulations in which box size was varied while keeping particle number fixed, indicates that there is a *weak* correlation between mass and spin at  $z=10$ , such that the spin decreases with increasing mass. If there is a correlation at  $z=1$ , we argue that it is significantly weaker than the one we find at  $z=10$ ; this is in qualitative agreement with the findings of previous studies that focused on lower redshifts (Maccio et al. 2007, Shaw et al. 2005, Lemson & Kauffmann 1999).

Interestingly, B07 find a weak correlation between median spin and halo mass at  $z=0$  in the Millennium Simulation (Springel et al. 2005), in the same spirit as the one presented here for  $z=10$ : lower mass halos tend to have higher spins. However, as we show, the correlation between halo mass and spin is weaker at  $z=1$  than at  $z=10$ , whereas the correlation reported in B07 for halos at  $z=0$  is much stronger than the one we find at  $z=1$ . This is not what one would expect, and so it is important to try and understand the source of the difference between our result at  $z=1$  and the B07 result at  $z=0$ . B07 fitted a 3<sup>rd</sup>-order polynomial to the median spins of halos in the mass range  $3 \times 10^{11} \lesssim M/(h^{-1}M_\odot) \lesssim 3 \times 10^{14}$  at  $z=0$ . The form of this polynomial is extremely sensitive to the precise values of the best-fit parameters (Bett, private communication) and it is not straightforward to extrapolate its behaviour outside of the given mass range and redshift. We derive our estimates of the power-law exponents from the spin distribution with respect to halo mass at  $z=1$ . Our halos lie in the mass range  $3 \times 10^9 \lesssim M/(h^{-1}M_\odot) \lesssim 5 \times 10^{12}$ . B07 base their median spins upon  $\sim 1.5$  million halos with correspondingly small errors, and note that the weak nature of the trend of spin with mass makes it hard to detect. This suggests to us that the correlation between mass and spin at  $z=10$  is remarkably strong rather than the correlation at  $z=1$  being too weak!

When studying correlations between halo mass and spin, great care must be taken in defining the halo sample. In particular, we find that mass resolution (i.e. the number of particles with which a halo is resolved) and the degree of virialisation of a halo can have a significant effect on the strength of the correlation (at least at  $z=1$ , cf. Table 5). This – at least – is in good agreement with the findings of B07.

We note that Power & Knebe (2006) demonstrated that the size of simulation box can lead to a suppression of angular momentum in smaller boxes, due to the absence of longer wavelength perturbations in the initial conditions. This will lead to a bias in our estimate of  $\lambda$  (approximately a  $\sim 10\%$  effect) but we have verified that the spin distributions we obtain from a B20 run truncated on scales larger than the longest wavelength perturbation modelled in the B1 run produces results that are consistent. Indeed, we would expect the correlation to be strengthened if the B1 spins were corrected for box size effects.

It is interesting to speculate on the consequences of this correlation for galaxy formation at high redshifts and the galaxy population we observe today. In the standard picture of galaxy formation, gas cools on to dark matter halos and is shock heated to the virial temperature of the halo. The angular momentum of the gas and the dark matter should (initially) be similar because they are subject to the same tidal field. As the innermost densest parts of the gaseous halo cool, they will settle into a gaseous

disk with a scale length determined by the specific angular momentum of the gas, which we would expect to be related to the angular momentum of the halo (e.g. Zavala, Okamoto & Frenk 2007).

If more massive halos at high redshifts show a tendency to have smaller spin parameters, the gas disks will have lower specific angular momenta and therefore will be more centrally concentrated. If star formation rate correlates with surface density, then we might expect the star formation rate to be enhanced in more massive halos. Because massive halos tend to form preferentially in high density, highly clustered environments in which the merger rate also tends to be enhanced, then we might expect star formation to proceed more rapidly and at earlier times in these halos. Might this explain the effect of “downsizing” (e.g. Cowie et al. 1996), the successive shifting of star formation from high- to low-mass galaxies with decreasing redshift? We shall pursue this in a more quantitative manner in future work.

AK would like to thank Swinburne University for its hospitality where this work was initiated. AK further acknowledges funding through the Emmy Noether programme of the DFG (KN 755/1). CP acknowledges funding through the ARC Discovery Projected funded “Commonwealth Cosmology Initiative”, grant DP 0665574. The simulations presented in this paper were carried out on the Beowulf cluster at the Centre for Astrophysics & Supercomputing, Swinburne University as well as the Sanssouci cluster at the Astrophysikalisches Institut Potsdam.

#### REFERENCES

- Barnes, J.; Efstathiou, G.; 1987, ApJ 319, 575  
 Bett, P.; Eke, V.; Frenk, C.S.; Jenkins, A.; Helly, A.; Navarro, J.; 2007, [astro-ph/0608607](#)  
 Bullock, J. S.; Dekel, A.; Kolatt, T. S.; Kravtsov, A. V.; Klypin, A. A.; Porciani, C.; Primack, J. R.; 2001, ApJ 555, 240  
 Cole, S.; Lacey, C.; 1996, MNRAS 281, 726  
 Cowie L.L., Songaila A., Hu E.M., Choen J.G., 1996, AJ 112, 839  
 Doroshkevich, 1979  
 Fall S. M. & Efstathiou G. 1980, MNRAS, 193, 189  
 Gao, L.; White, S.D.M.; 2007, MNRAS 377, L5  
 Gardner, J.P.; 2001, ApJ 557, 616  
 Gill, S.P.D.; Knebe, A.; Gibson, B.K.; 2004, MNRAS 351, 399  
 Gottloeber S., Yepes G., 2007, ApJ 664, 117  
 Gross, M.A.K., 1997, PhD thesis Univ. California, Santa Cruz  
 Hetzner, H.; Burkert, A.; 2006, MNRAS 370, 1905  
 Knollmann S., Power C., Knebe A., 2008, MNRAS accepted  
 Lemson, G.; Kauffmann, G.; 1999, MNRAS 302, 111  
 Maccio, A.V.; Dutton, A.A.; van den Bosch, F.C.; Moore, B.; Potter, D.; Stadel, J.; 2007, MNRAS 378, 55  
 Maller, A.H.; Dekel, A.; Somerville, R.; 2002, MNRAS 329, 423  
 Mo, H.J.; Mao, S.; White, S.D.M.; 1998, MNRAS 295, 319  
 Navarro J.F., Frenk C.S., White S.D.M., 1997, ApJ 490, 493  
 Neto A.F., et al., [astro-ph/0706.2919](#)  
 Peebles J.; 1969  
 Power, C.B.; Knebe, A.; Knollmann, S.; 2008, MNRAS submitted  
 Porciani; Dekel; Hoffman; 2002  
 Shaw, L.D.; Weller, J.; Ostriker, J.P.; Bode, P.; 2006, ApJ 646, 815  
 Spergel, D.; et al.; 2003  
 Springel, V.; et al.; 2005, Nature 435, 629  
 Sugerman; Summers; Kamionkowski; 2000  
 Vitvitska, M.; Klypin, A.A.; Kravtsov, A.V.; Wechsler, R.H.; Primack, J.R.; Bullock, J.S.; 2002, ApJ 581, 799  
 White, S.D.M. & Rees, M. 1978, MNRAS, 183, 341  
 White, S.D.M.; 1984  
 Zavala J., Okamoto T. & Frenk. C. S. [astro-ph/0710.2901](#)

TABLE 1  
SUMMARY OF THE COSMOLOGICAL SIMULATIONS AND NUMBER OF HALOS.

run	$L_{\text{box}} [h^{-1} \text{ Mpc}]$	$m_p [h^{-1} M_{\odot}]$	$z_{\text{final}}$	$N_{\text{halos}}^{z=1}$	$N_{\text{halos}}^{z=10}$	$N_{\text{relaxed halos}}^{z=1}$	$N_{\text{relaxed halos}}^{z=10}$
B01	1	$4.9 \times 10^3$	10	—	8780	—	286
B02	2.5	$7.8 \times 10^4$	10	—	7991	—	201
B05	5	$6.2 \times 10^5$	1	16917	6532	832	109
B10	10	$4.9 \times 10^6$	1	18589	4360	949	37
B20	20	$4.0 \times 10^7$	1	20514	10947	995	27
B100	100	$4.9 \times 10^9$	1	24696	—	978	—

TABLE 2  
FITTING PARAMETERS FOR  $P(\lambda)$ .

run	$\lambda'_0$	$\sigma$	$\lambda'_{\text{med}}$	$M_{\text{med}} [h^{-1} M_{\odot}]$	run	$\lambda'_0$	$\sigma$	$\lambda'_{\text{med}}$	$M_{\text{med}} [h^{-1} M_{\odot}]$
			$z=1$					$z=10$	
			—		B01	0.042	0.538	0.041	5.95e+06
			—		B02	0.040	0.539	0.037	8.19e+07
B05	0.033	0.521	0.031	7.92e+08	B05	0.036	0.516	0.035	5.63e+08
B10	0.037	0.527	0.034	6.15e+09	B10	0.033	0.540	0.029	4.14e+09
B20	0.038	0.543	0.036	5.40e+10	B20	0.030	0.251	0.027	3.33e+10
B100	0.037	0.535	0.035	5.25e+12				—	

TABLE 3  
VARIATION OF  $\alpha$  WITH  $N_{\text{bins}}$  ( $Q_{\text{lim}} = 0.15, N_{\text{min}} = 600$ ).

$N_{\text{bins}}$	$\alpha_{z=1} \pm \sigma_{\alpha}$	$\alpha_{z=10} \pm \sigma_{\alpha}$
4	$-0.001 \pm 0.169$	$-0.061 \pm 0.191$
5	$-0.002 \pm 0.149$	$-0.059 \pm 0.171$
6	$-0.005 \pm 0.137$	$-0.053 \pm 0.155$
7	$-0.006 \pm 0.128$	$-0.056 \pm 0.144$
8	$-0.003 \pm 0.120$	$-0.069 \pm 0.132$

TABLE 4  
VARIATION OF  $\alpha$  WITH  $Q_{\text{lim}}$  ( $N_{\text{bins}} = 5, N_{\text{min}} = 600$ ).

$Q_{\text{lim}}$	$\alpha_{z=1} \pm \sigma_{\alpha}$	$\alpha_{z=10} \pm \sigma_{\alpha}$	$N_{\text{relaxed halos}}^{z=1}$	$N_{\text{relaxed halos}}^{z=10}$
0.05	$-0.007 \pm 0.148$	$-0.058 \pm 0.153$	2123	264
0.10	$-0.004 \pm 0.148$	$-0.062 \pm 0.168$	3365	497
0.15	$-0.002 \pm 0.149$	$-0.059 \pm 0.171$	3811	660
0.20	$-0.005 \pm 0.151$	$-0.052 \pm 0.173$	3994	739
0.25	$-0.002 \pm 0.153$	$-0.052 \pm 0.173$	4165	774

TABLE 5  
 VARIATION OF  $\alpha$  WITH  $N_{\min}$  ( $Q_{\text{lim}} = 0.15, N_{\text{bins}} = 5$ ).

$N_{\min}$	$\alpha_{z=1} \pm \sigma_{\alpha}$	$\alpha_{z=10} \pm \sigma_{\alpha}$	$N_{\text{relaxed halos}}^{z=1}$	$N_{\text{relaxed halos}}^{z=10}$
100	$0.003 \pm 0.129$	$-0.037 \pm 0.158$	19707	5478
200	$0.002 \pm 0.137$	$-0.038 \pm 0.167$	10809	2534
300	$0.002 \pm 0.142$	$-0.035 \pm 0.174$	7336	1526
600	$-0.002 \pm 0.149$	$-0.059 \pm 0.171$	3811	660
1000	$-0.004 \pm 0.155$	$-0.058 \pm 0.196$	2303	343
2000	$-0.011 \pm 0.164$	$-0.048 \pm 0.186$	1154	120

TABLE 6  
 APPLYING DIFFERENT VIRIALISATION CRITERION ( $N_{\text{bins}} = 5$ ).

critierion	$\alpha_{z=1}$	$\alpha_{z=10}$	$N_{\text{relaxed halos}}^{z=1}$	$N_{\text{relaxed halos}}^{z=10}$
Neto et al. (2007)	$0.000 \pm 0.149$	$-0.041 \pm 0.178$	3486	429
Maccio et al. (2007)	$0.001 \pm 0.146$	$-0.040 \pm 0.184$	4275	512
Bett et al. (2007)	$0.003 \pm 0.146$	$-0.040 \pm 0.175$	8582	1955

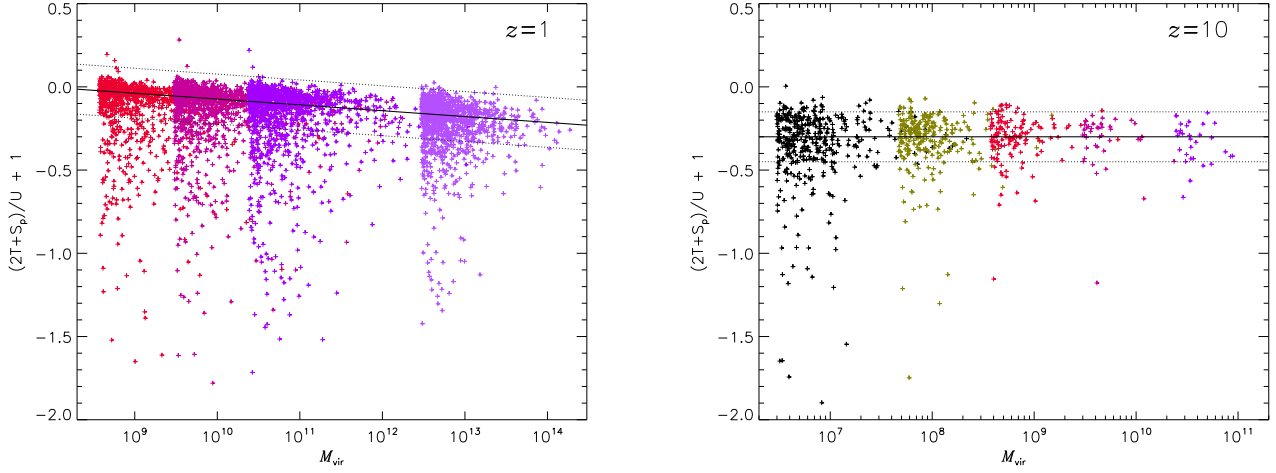


FIG. 1.— Relation between virial parameter  $Q$  (cf. equation 3) and halo mass. The solid lines represent the adopted virialisation criteria as given by Eq. (4). Note that we already applied the mass cut of 600 particles per halo for this plot and hence the number of halos appearing does not agree with the number given in Table 1.

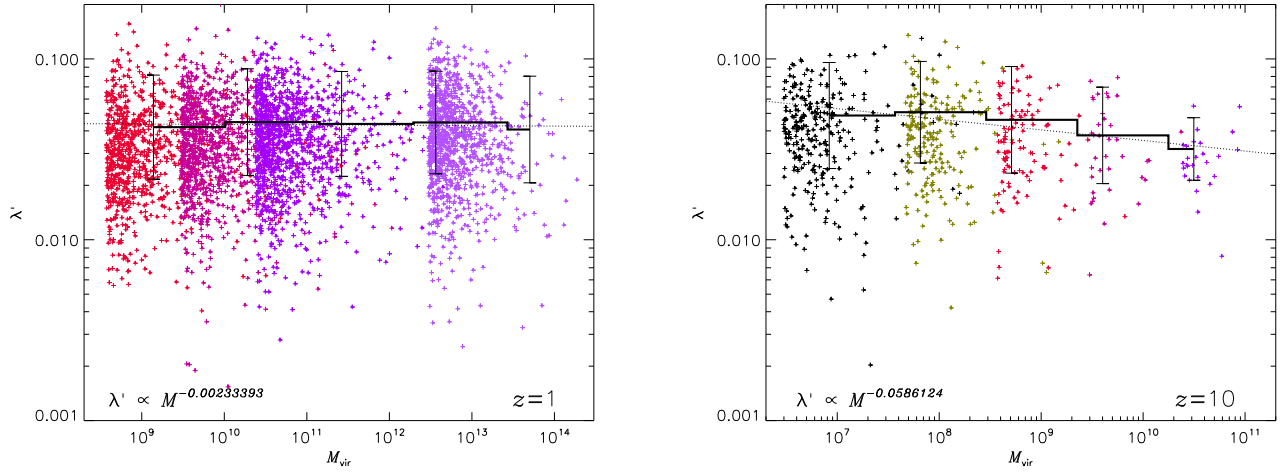


FIG. 2.— Correlation of spin parameter  $\lambda$  with mass  $M$ . The binned data (histograms) has been fitted to a power laws (dashed line, cf. Eq. (9)).

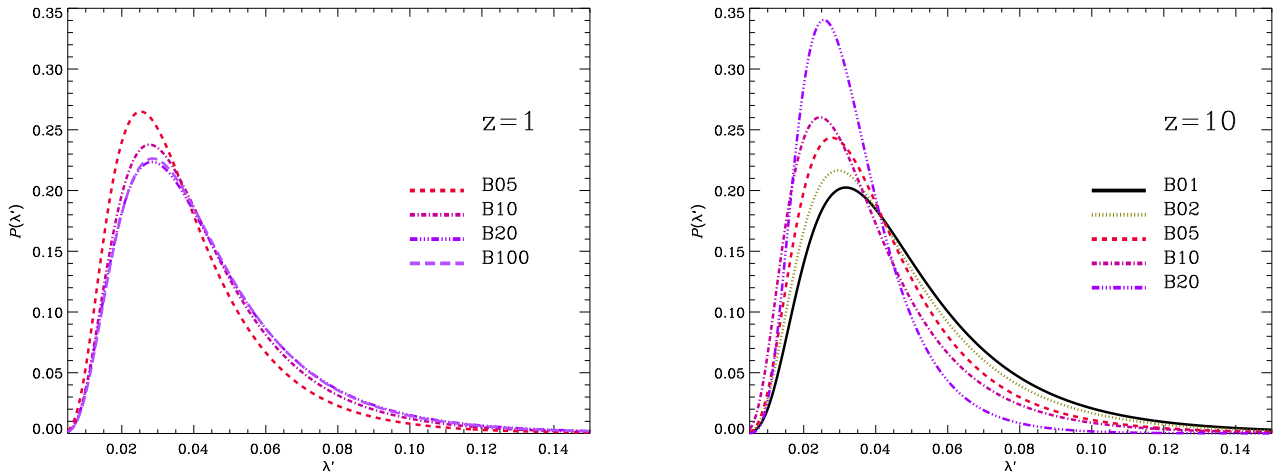


FIG. 3.— Lognormal distributions of the spin parameter  $\lambda'$ .